Impact of vehicle propulsion electrification on well-to-wheel CO_2 emissions of a medium duty truck

Tomaž Katrašnik

University of Ljubljana, Faculty of Mechanical Engineering, Aškerčeva 6, SI-1000 Ljubljana, Slovenia; tel.: +386 1 4771 305, e-mail: tomaz.katrasnik@fs.uni-lj.si

Abstract

Well-to-Wheel (WtW) CO_2 emissions of different powertrain topologies employed to power a medium duty truck are analyzed in this paper. The analysis covers topologies of the parallel and the series plug-in hybrid electric vehicles (PHEV), which are driven according to different strategies of depletion of the electric storage devices (ES). These results are benchmarked against results of conventional internal combustion engine vehicles (ICEV). The Tank-to-Wheel (TtW) data are obtained by a forward facing vehicle simulation model, whereas Well-to-Tank (WtT) analysis covers CO_2 intensity of the Diesel fuel and four different realistic CO_2 intensities of electric energy production. To ensure comprehensiveness of the study vehicles were also operated according to two drive cycles that feature significantly different velocity profiles. In addition, influences of different control strategies of powertrain components were also analyzed. This broad portfolio of scenarios reveals insightful WtW CO_2 emissions guidelines for introducing plug-in hybrid electric trucks to different regions. The results indicate that the propulsion electrification in medium duty trucks has, in comparison to passenger cars, a smaller potential for reduction of Well-to-

Wheel CO_2 emissions because of the higher efficiencies of the internal combustion engine in such trucks. Results of this study were also used to identify the threshold value of the CO_2 intensity of electric energy production that favors the operational switch from Charge Depleting (CD) to Charge Sustaining (CS) mode. Additionally, it was shown that for longer recharge intervals, operation in the blended mode with less intensive depletion rate of the ES can feature lower WtW CO_2 emissions of the PHEVs.

Keywords: PHEV; ICEV; medium duty truck; transient drive cycle; WtW CO_2 emissions; realistic CO_2 intensities of electric energy production

Nomenclature:

d	length of the drive cycle (m)
E_{CO_2}	energy specific CO_2 emissions (gCO_2eq/MJ)
l	length of the trip, recharge interval (m)
$M^*_{CO_2}$	instantaneous distance specific CO_2 emissions (gCO_2eq/km)
M_{CO_2}	integrated distance specific CO_2 emissions (gCO_2eq/km)
m	mass (kg)
Q_{LHV}	lower fuel heating value (J/kg)
t	time (s)
$t_{0-50km/h}$	acceleration time from stand still to 50 km/h (s)
$t_{0-100km/h}$	acceleration time from stand still to 100 km/h (s)
v	velocity (m/s)
x	distance (m)
W	energy (J)

η	efficiency (-)

Subscripts and abbreviations:

CD	charge depleting
CS	charge sustaining
dc	drive cycle
DoD	depth of discharge
EL	electric energy
EM	electric machine
ES	electric storage
EV	electric vehicle
F	fuel, fuel tank
HEV	hybrid electric vehicle
HF	hybridization factor
ICE	internal combustion engine
ICEV	vehicle driven by an internal combustion engine
L	load
p	parallel
PHEV	plug-in hybrid electric vehicle
PR	propulsion
s	series
SOC	state of charge
StSt	start-stop
TtW	tank-to-wheels
W	wheel

WtT	well-to-tank
WtW	well-to-wheel

1. Introduction

Currently many production and prototype vehicles as well as the results of research studies, e.g. [1-6], demonstrate that hybrid-electric vehicles (HEVs) attain better fuel economy and lower exhaust emissions compared to conventional internal combustion engine vehicles (ICEVs) in the majority of vehicle applications and in the majority of vehicle's operating conditions. Plug-in hybrid-electric vehicles (PHEVs) have brought this concept to a higher level by offering the functionality to draw the electric power for vehicle propulsion also from the electric grid. This functional change from the conventional HEVs allows a PHEV to displace energy from petroleum with multi-source electric energy [7]. PHEVs do therefore not only have potential to further reduce energy consumption and exhaust emissions compared to HEVs and ICEVs (as presented in e.g. [8-13]) but they also enable the use of the energy from sources other than crude oil [14], which is the main source of liquid hydrocarbon fuels. The mix of energy sources used to produce the electric energy and their pathways most significantly influences potential benefits of the PHEVs in terms of CO_2 emissions [14].

The reduced CO_2 emissions of PHEVs have already been studied in the literature. The majority of the studies aimed at predicting national or fleet energy demands or electricity demands to charge the PHEVs, e.g. [11-19], and evaluating total cost of ownership [20] rely on simulation models that use cycle or fleet averaged efficiency and energy consumption data. In Ref. [21] the cost and emissions impacts of PHEVs were analyzed using a backward facing simulation model that uses map based inputs of component characteristics. This modeling depth was also used in [22] to investigate the efficiency of different range extending systems and in [23] to model prospects of plug-in hybrid electric vehicles to reduce

CO_2 emissions of a particular vehicle type. In contrast to the above referenced studies, the study in [8] is based on a forward-facing model capable of accepting a command from the driver. This model also uses map based component models. The benefits and deficiencies of different modeling approaches of HEVs that also serve as the basis for modeling PHEVs are presented and compared in [24]. There it is reasoned that the forward facing models are clearly favorable for the analyses of a single vehicle type.

The above mentioned studies focus primarily on passenger cars. In addition, Ref. [15] states that the medium and heavy duty vehicles significantly contribute to the overall CO_2 emissions in transport. Medium and heavy duty vehicles feature different powertrain and vehicle characteristics compared to passenger cars, which inherently leads to different operating regimes of powertrain components. Therefore, this paper analyses the impact of vehicle propulsion electrification on WtW CO_2 emissions of a medium duty truck and highlights specific emission trends related to this vehicle type. As the study aims at analyzing CO_2 emissions of series and parallel PHEV topologies used under different driving and charging scenarios, it focuses on a single vehicle type that is modeled with a forward facing simulation model. This is necessary to adequately capture the interaction between different driving patterns and parameters of the powertrain that are influenced by the PHEV topology and state of charge (SOC) of ES. Because medium and heavy duty vehicles are powered by Diesel engines that are nearly exclusively turbocharged, a mechanistic system level engine model is used in this study to efficiently capture the transient response of the turbocharged engine. This is important because the dynamic response of the turbocharger significantly influences the power output of the engine, which features much larger response time in terms of power output than other components of the PHEV powertrains. This is of particular importance in parallel PHEVs, where the engine is subjected to transient operating conditions

and thus correct value of the engine power output is needed to adequately model power split between the components.

The study is thus aimed at comparing WtW CO_2 emission of a medium duty truck featuring ICEV and PHEV powertrain topology, where PHEV topology is operated with different depletion rates of the ES. In addition, the analysis considers different realistic CO_2 intensities of electric energy production, which reveals insightful guidelines for introduction of plug-in hybrid electric trucks to different regions.

2. Methodology

2.1. Simulation model

For the purpose of this study a forward-facing model presented in [6] was used to model the ICEV (Fig. 1). Both PHEV topologies (Fig. 1) were simulated by a model presented in [9] that also gives detailed description of sub-models of control strategies for PHEVs. The model for simulating PHEVs was derived by extending the model of HEVs [6]. Ref. [6] also presents models for modeling vehicle dynamics. Details on the models of propulsion units of the vehicles, i.e. powertrains, are presented in [24,25]. Subsequently, to preserve brevity of the model description, the modeling approach is briefly summarized.

2.1.1 Sub-models and parameters of vehicle and powertrain components

Analyses were performed for a MAN 8.225 LC 7490 kg gross weight truck powered by a MAN D0826 LOH 15 turbocharged diesel engine (max. torque 862Nm at 1400rpm, max. power 158kW at 2400 rpm and effective efficiency of 44% in the range from 800 to 1300 rpm and above approx. 380 Nm) and equipped by a six gear S6–850 gearbox representing a baseline ICEV [6]. When modeling PHEVs, maximum payload was preserved, whereas mass increase due to additional batteries, electric machines and other electric accessories as well as

mass decrease due to downsizing ICE in both of the two PHEV topologies and omission of the gear box in the series PHEV is taken into account as discussed in [6]. Basic data of ICEV and parallel PHEV (pPHEV) and series PHEV (sPHEV) are given in Table 1.

Both PHEVs employ downsized ICEs featuring 50% of the swept volume of the baseline ICE. EM in the sPHEV (EM1) was sized so that that its maximum power output corresponds to the power of the baseline ICE at maximum torque output, i.e. 862 Nm at 1400 rpm giving 126.4 kW – Table 1 [6]. EM in a pPHEV was sized so that that combined power of the downsized ICE and EM1 again equals to the power of the baseline ICE at engine speed corresponding to maximum torque resulting in hybridization factor HF=0.464 [6]. Characteristics and the scaling procedure of the EM1 in pPHEV and sPHEV are given in [24] and characteristics of the EM2 in sPHEV are given in [6,25].

ICE is characterized by a torque decrease below 1400 rpm, i.e. engine speed that corresponds to maximum torque, whereas contrary, EM1 features constant maximum torque below 1200 rpm [24]. Therefore, in comparison to the ICEV both PHEVs feature higher power outputs of propulsion unit(s) below 1400 rpm and lower power outputs above 1400 rpm. Despite the inherent differences in the characteristics of power units the analyzed vehicles feature similar maximum vehicle velocities (variations of less than 6%) with ICEV being the fastest one. PPHEV is further characterized by the shortest acceleration time from stand still to 50 km/h ($t_{0-50km/h}$ - Table 1) due to the high power output of the powertrain at lower speeds, whereas its acceleration time from stand still to 100 km/h ($t_{0-100km/h}$) does not differ much from the one of ICEV due to the lower power outputs of the powertrain above 1400 rpm (exact trends are based on the gear shift strategy as discussed in [26] that deals with very similar parallel powertrain configuration). Unlike the PPHEV, the SPHEV features longer acceleration times from stand still (Table 1) despite the highest torque output of the EM1 at low speeds. This is due to the selection of the gear ratio in a single ratio transmission

which was selected in a way to ensure a sufficiently high maximum vehicle velocity. The application of a single ratio transmission does not notably influence the energy conversion efficiency during the analyzed driving cycles, whereas if vehicle acceleration performance were to be optimized it would be beneficial to choose a gear box with two gears ensuring comparable acceleration times to the other two topologies.

The simulation model of the ICE is based on the 0-D filling and emptying method [27]. The capability of the ICE model to accurately model steady-state and transient operation of the baseline ICE is shown in [27] and briefly recapitulated in [24]. EMs were modeled based on the experimentally determined characteristics. Drivetrain models use manufacturer's performance characteristics as inputs of the model [6], whereas rolling resistance momentum of the tires was modeled according to the model proposed in [28].

Both PHEVs apply ENAX Li-Ion High Power Li-Ion batteries as ES [5]. The battery model uses manufacturer's performance characteristics as inputs of the model [5]. Battery stack was sized to meet the requirements on the trade-off between minimum added mass due to powertrain electrification and sufficient range in the CD mode. In addition safety constraints that predominantly cover not exceeding maximum charging and discharging currents of the batteries at maximum performance of the EM/s were taken into account.

Validation of the capability of the driver model to accurately follow the vehicle velocity trace given by the drive cycle is presented in [6]. Ref. [6] also shows the gear shifting strategy, which is applied in the ICEV and pPHEV.

In this study both PHEV topologies were also driven with neutral SOC of electric storage devices to analyze their performance in cases of long range driving or long recharge intervals. This operation mode is denoted as HEV, because in this case PHEV operates in the CS mode, i.e. initial and final SOC are equal for a particular drive cycle or a particular driving segment (ΔW_{ES}^{*} =0). Therefore, subsequently notation PHEV refers to the operation mode where

$\Delta W_{ES}^{*} > 0$ and notation HEV refers to specific operating conditions of the PHEV where $\Delta W_{ES}^{*} = 0$.

2.2. Drive cycles

All vehicle topologies were driven according to the BUSRTE (2.65-km bus route with 28 stops) and UDDSHDV (Urban Dynamometer Driving Schedule for Heavy-Duty Vehicles) drive cycle shown in Fig. 2. BUSRTE [29] is a real-world driving cycle representative of an urban bus, which might also mimic driving conditions of a refuse or delivery truck. UDDSHDV [30] is a standardization cycle proposed by EPA. BUSRTE features low average velocity and frequent decelerations to stand-still. BUSRTE has thus potential for significant recuperation of energy by regenerative braking. UDDSHDV is a highly transient cycle with frequent accelerations/decelerations including high velocity segments. Average velocity of UDDSHDV is much higher than average velocity of BUSRTE. For the analyzed ICEV (Table 1) the average specific energy needed for vehicle propulsion (W_{PR}) equals 337.6 J/km/kg and 286.3 J/km/kg for the BUSRTE and UDDSHDV cycle respectively and the average specific energy needed for decelerating the vehicle equals 320.8 J/km/kg and 95.6 J/km/kg for the BUSRTE and UDDSHDV cycle respectively, where unit J/km/kg denotes energy given to or extracted from the load, i.e. road, per unit distance driven and per unit vehicle mass. The two drive cycles differ significantly in terms of the energy needed for vehicle propulsion and energy needed for decelerating the vehicle. These two drive cycles were therefore chosen to analyze the drive cycle specific influences on the WtW CO2 emissions, as they cover a wide range of application areas.

2.3. Operating modes of the vehicles

The ICEV is operated in two modes, i.e. with and without start-stop strategy, as presented

in [6]. These two sets of data are used to benchmark impact of vehicle propulsion electrification on WtW CO_2 emissions.

Based on the power outputs of the electric components (Table 1) sPHEV is capable of operating in pure EV mode during CD operation, as EM1 is the only vehicle propulsion unit and ES are sized in a way not to restrict operation of the EM. Unlike the sPHEV, pPHEV operates in blended mode during CD operation mode, as power output of the EM1 is not sufficient to propel the vehicle during fast accelerations at high speeds. Details and reasoning of the applied heuristic control strategy are presented in [9] with a brief summary presented below.

Two different regimes of vehicle propulsion for drive-away and low powertrain loads were analyzed for the pPHEV [9]: (1) ICE solely provides the torque for vehicle propulsion up to maximum torque output of the ICE, and (2) EM solely provides the torque up to a specific power limit (it is defined as $\min\left(P_{EM1,\max}, P_{EM,assist,\max}\right)$); $P_{EM,assist,\max} = 30kW$ to preserve high overall energy conversion efficiency [6]) and afterwards ICE solely provides the torque for vehicle propulsion up to maximum torque output of the ICE. The second control strategy is denoted EMS and suffix "_EMS" is added to identify this operation mode in the figures, whereas if no specific notation is used operation refers to the first control strategy of the pPHEV. At higher power requirements both the ICE and the EM provide the power for propulsion in pPHEV. If EMS control strategy is applied to the pPHEV during the UDDSHDV drive cycle it is not possible to fulfill the condition ΔW_{ES}^{*} =0 as presented in [9], i.e. it is not possible to drive the vehicle in the CS mode. Therefore results of the EMS strategy were not analyzed in this paper for the UDDSHDV drive cycle. However, results of both control strategies were analyzed for the BUSRTE drive cycle to show differences in WtW CO_2 emissions due to different control strategies. Drive cycles that feature significant potential for energy recuperation by regenerative braking namely favor utilization of electric

propulsion pathway to increase energy conversion efficiency of the hybrid powertrains.

The ICE of the series PHEV was operated according to the optimum engine operation line (OEOL) [9]. OEOL is constituted of engine speed and torque points in the high engine efficiency region, i.e. it follows the maximum torque curve with some operational safety margin. In the presented analysis the ICE and thus also EM2 were controlled by the state-of-charge (SOC) of ES and drive cycle characteristics. In addition, ICE was turned off below a minimum ICE power threshold to avoid inefficient operation of the engine-generator unit.

In this study maximum depth of discharge (DoD) of ES is 65%, which is average of a more moderate DoDs of around 60%, e.g. [23], and more aggressive DoDs of around 70%, e.g. [18]. A shift from CD to CS mode is performed at 0.3 SOC of the ES. However, values of the SOC when operating in the HEV mode are not constantly 0.3, as exact values of the neutral SOC depend on the interaction between the drive cycle, powertrain parameters and control strategy as indicated by different values for the pPHEV and sPHEV in Fig. 3.

With DoD of 65% sPHEV features 19.9 km range in the CD operation for the UDDSHDV and 26 km range in the CD operation for the BUSRTE, where CD operation corresponds to the pure EV mode. With the same DoD pPHEV features 20.1 km range in the CD operation for the UDDSHDV and 40.7 and 81.4 km range in the CD operation for the BUSRTE, where the two figures correspond to the two cases where EMS is enabled and disabled respectively. For the pPHEV CD operation corresponds to the blended mode. If EMS is disabled, pPHEV features very long range in the CD mode for the BUSRTE drive cycle because the significant amount of the energy that is recuperated by the regenerative braking is used for propulsion only in cases where power demand exceeds the power output of the ICE. The ranges of the PHEVs in the CD mode indicate that battery size is applicable to urban delivery truck with the fast charge option and it represents a good compromise between additional mass, cost and the amount of the stored electric energy. Moreover, due to moderate increase of system mass

both PHEVs feature acceptable energy consumption also during longer driving cycles, where they are operated predominately in the CS, i.e. HEV, mode. This is particularly true for the pPHEV, as it features relatively low vehicle mass and mechanical connection between the engine and the wheels. The latter namely positively influences energy conversion efficiency of the pPHEV during driving cycles featuring elevated velocities and relatively high power demands.

In this study both PHEV topologies are analyzed for different depletion rates of the ES, as depletion rate of the ES influences energy conversion efficiency of PHEVs [9] and thus also its WtW CO_2 emissions. Operation of the PHEVs according to different depletion rates is achieved by starting drive cycles with different initial energy contents of the ES and preserving identical control strategy.

2.4. WtW analysis

WtW analysis is based on the TtW energy consumption data, which are calculated by the simulation model presented in section 2.1 and WtT data from the literature. For the Diesel fuel both CO_2 emissions, i.e. WtT ($E_{WtT,CO_2,F}$) and TtW ($E_{TtW,CO_2,F}$), contribute to the WtW emissions ($E_{WtW,CO_2,F} = E_{WtT,CO_2,F} + E_{TtW,CO_2,F}$), whereas for electric energy only WtT ($E_{WtT,CO_2,EL}$) emissions contribute to the WtW emissions ($E_{WtW,CO_2,EL} = E_{WtT,CO_2,EL}$).

For the Diesel fuel, CO_2 emissions data were obtained from [31] and amount to 15.9 and 73.25 gCO_2eq/MJ for WtT and TtW respectively. The first value considers contributions of crude oil extraction and processing, crude oil transport, its refining and its distribution and dispensing, whereas the second value corresponds to combustion of the Diesel fuel in the engine.

Four different CO_2 intensities of electric energy production are considered in the analysis to expose a very large impact of WtT CO_2 emissions of electric energy production on the total

WtW emissions of the PHEVs. CO_2 intensities of electric energy production for France, European Union, USA and China were obtained from [32] and amount to 24.4, 112.2, 169.6 and 241.1 gCO_2eq/MJ respectively. This was done on one hand to highlight results of realistic scenarios and on the other to serve as a kind of sensitivity analysis indicating which topologies and which operating regimes of PHEVs exhibit large sensitivity to WtT CO_2 intensity of electric energy production. WtT CO_2 emissions were obtained considering CO_2 intensities of electric energy production, transmission and distribution losses of the electric energy (8% [19]) and charging efficiency of ES (94% [9,23,33]).

Constant CO_2 data are used for the fuel, as it is not possible to accurately determine variations in fuel processing and share of biofuels. Moreover, only CO_2 emissions related to driving the vehicle are considered and not the total life-cycle CO_2 emissions of the vehicle.

The WtW CO_2 emissions are thus analyzed as a function of the driven distance, which is denoted as distance specific WtW CO_2 emissions - M_{WtW,CO_2}. Basis input of this calculation are thus energy depleted from the fuel tank ($\Delta W_F = \Delta m_F Q_{LHV}$) and energy depleted from the batteries (ΔW_{ES}^*), where the first one is zero for the PHEV operating in pure EV mode and the second one is zero for the ICEV and HEV. Based on the known values of these two parameters mass of WtW CO_2 emissions for a specific drive cycle or a specific driving segment (dc) is calculated as

$$m_{WtW,CO_2,dc} = \Delta W_F E_{WtW,CO_2,F} + \Delta W_{ES}^* E_{WtW,CO_2,EL} . \quad (1)$$

Eq. (1) can be used to evaluate distance specific WtW CO_2 emissions considering the length of the particular drive cycle or particular driving segment (dc)

$$M_{WtW,CO_2}^* = \frac{m_{WtW,CO_2,dc}}{d} . \quad (2)$$

M_{WtW,CO_2}^* values of the ICEVs are HEVs are not dependent on the CO_2 intensity of electric energy production as for these vehicles the only external energy source is fuel, i.e. the second

term in eq. (1) is zero. M^{*}_{WtW,CO_2} values of the ICEVs and HEVs are therefore also distance independent for particular driving conditions. On the contrary, M^{*}_{WtW,CO_2} of the PHEVs depends on the depletion rate of on-board energy sources, since PHEV start operating in the CD mode after they are recharged and later switch to the CS mode. Therefore, M^{*}_{WtW,CO_2} of the PHEVs depend on the driven distance

$$M^{*}_{WtW,CO_2}(x) = \begin{cases} M^{*}_{WtW,CO_2,CD}; \text{in CD mode} \\ M^{*}_{WtW,CO_2,CS}; \text{in CS mode} \end{cases}. \quad (3)$$

Total WtW CO_2 emissions of the PHEVs over a recharge interval l are thus evaluated as

$$M_{WtW,CO_2} = \frac{\int_o^l M^{*}_{WtW,CO_2}(x)\mathrm{d}x}{l}. \quad (4)$$

According to the above definition, when PHEV operates in the CS, i.e. HEV, mode its WtW CO_2 emissions (M_{WtW,CO_2}) equal $M^{*}_{WtW,CO_2,CS}$. Similarly, according to eqns. (3) and (4) it can be concluded that for large l, M_{WtW,CO_2} of the PHEV approaches $M^{*}_{WtW,CO_2,CS}$, i.e. WtW CO_2 emissions of the PHEV approach those characteristic for the operation in the CS mode.

3. Results

This section focuses on the WtW CO_2 emissions by first analyzing powertrain data and energy consumptions, which form the inputs for the WtW CO_2 analyses. Detailed analysis on the energy conversion phenomena of the investigated ICEVs is given in [6] and analysis on the energy conversion phenomena of PHEVs and HEVs is given in [9]. The following notation is used in this section:

pPHEV: parallel plug-in hybrid electric vehicle;

sPHEV: series plug-in hybrid electric vehicle;

pHEV: pPHEV operated according to the HEV mode, i.e. $\Delta SOC = 0$;

sHEV: sPHEV operated according to the HEV mode, i.e. $\Delta SOC = 0$;

ICEV: internal combustion engine vehicle without start-stop strategy and

ICEV_StSt: internal combustion engine vehicle with start-stop strategy.

The additional "_EMS" indicates operation of the pPHEV or pHEV according to the EMS strategy for the BUSRTE drive cycle as presented in section 2.3.

3.1. Results of different operating modes of PHEVs

Fig. 3 shows SOC and $m_{F,dc}$ (mass of the fuel consumed over the drive cycle) of the sPHEV and pPHEV driven according to the UDDSHDV drive cycle for different initial values of the SOC. sPHEV operates in pure EV mode for initial value of SOC=0.7 or higher because $m_{F,dc}$=0 over the complete drive cycle. Energy for vehicle propulsion is thus gained only by depleting the ES. However, for initial SOC=0.278 sPHEV operates entirely in the CS mode with ΔW_{ES}^{*}=0, which corresponds to the HEV operation. This is indicated by higher fuel consumption ($m_{F,dc}$) over the whole drive cycle. For intermediate SOCs sPHEV at first operates as pure EV in CD mode and afterwards in the CS mode. To ensure readability of the figures, ICE on/off mode is not shown in the figures, however this information is discernible from the results of $m_{F,dc}$: regions with $\mathrm{d}m_{F,dc}/\mathrm{d}t > 0$ indicate that the ICE is turned on and regions with $\mathrm{d}m_{F,dc}/\mathrm{d}t = 0$ indicate ICE turned off.

Results of fuel consumption of the pPHEV indicate that pPHEV operates in the blended mode during CD operation because EM1 is not sufficient powerful as discussed in section 2.3. This is indicated by the fact that during CD operation besides SOC decrease also increase in $m_{F,dc}$ can be observed for the case with initial SOC=0.6 of the pPHEV (Fig. 3). Different SOCs certainly influence the power split between ICE and EM1, favoring more intensive

usage of electric energy at higher SOC. The latter is indicated by different slopes of curves representing $m_{F,dc}$ and SOC when comparing the two pPHEVs with initial SOC=0.6 and 0.31.

3.2. Powertrain parameters

Fig. 4 shows energy extracted from both on board energy storage devices (fuel tank and batteries) multiplied by the efficiency of the corresponding energy conversion paths (denoted $W_{F,ES\to L}$) for the UDDSHDV cycle. Efficiencies of the energy conversion paths from F to L (η_{F-L}) and from ES to L (η_{ES-L}) are defined as a product of efficiencies of all elements in the corresponding energy conversion path (Fig. 1). $W_{F,ES\to L}$ can thus be defined as

$$W_{F,ES\to L} = W_{F\to L} + W_{ES\to L} = \Delta W_F \eta_{F-L} + \Delta W_{ES}^{*} \eta_{ES-L} = \Delta m_F Q_{LHV} \eta_{F-L} + \Delta W_{ES}^{*} \eta_{ES-L} . \quad (5)$$

While considering the load as the origin for the evaluation of the energy conversion phenomena, $W_{F,ES\to L}$ gives the combined information on: 1.) the amount of energy that is used for vehicle propulsion, 2.) the amount of the energy that was recuperated by the regenerative braking and used for vehicle propulsion, 3.) the amount of the energy loses due to charging the batteries by operating the ICE at higher power output and 4.) the amount of the energy consumed by the ICE during motoring in the pPHEV. Another parameter that substantially influences energy consumption is the energy needed for vehicle propulsion (W_{PR}), where W_{PR} considers only the positive values of the traction force [34]. Therefore, combined analysis of the $W_{F,ES\to L}$ and W_{PR} provides insight into the trade-off between positive influences due to regenerative braking and negative influences due to the losses under item 3.) and 4.) in the previous sentence.

For the UDDSHDV the values of W_{PR} equal 20.1 and 19.4 MJ for sPHEV and pPHEV respectively. $W_{F,ES\to L}$ (Fig. 4) features lower values than W_{PR} mainly due to benefits

associated with regenerative braking. In Fig. 4 data are plotted as a function of $\Delta\mathrm{SOC} = \mathrm{SOC}_{\mathrm{init}} - \mathrm{SOC}_{\mathrm{final}}$ and thus $\Delta\mathrm{SOC}=0$ corresponds to HEV, whereas in subsequent figures it also corresponds to ICEVs. Fig. 4 additionally shows that value of $W_{F,ES\rightarrow L}$ increases for decreasing $\Delta\mathrm{SOC}$. This $W_{F,ES\rightarrow L}$ trend is mainly related to the increased losses due to charging the ES by operating the ICE at higher power output, which is required to sustain the SOC [9]. By comparing results of the pPHEV and sPHEV it can be concluded that sPHEV features lower value of $W_{F,ES\rightarrow L}$ at $\Delta\mathrm{SOC}=0$ due to smaller losses associated with charging the ES by operating the ICE at higher power output, whereas it features higher value of $W_{F,ES\rightarrow L}$ for larger values of $\Delta\mathrm{SOC}$ due to larger vehicle mass and thus larger value of W_{PR}. Different trend can be observed for the BUSRTE cycle, which offers a substantial amount of energy for replenishing of the ES through the regenerative braking (Section 2.2). Therefore, ES are never charged by operating the ICE at higher power output for the BUSRTE cycle. This results in nearly constant $W_{F,ES\rightarrow L}$ value of 4.65 and 4.6 MJ for different DoDs, i.e. $\Delta\mathrm{SOC}$, and W_{PR} value of 6.8 and 7.1 MJ for the parallel and series topology respectively [9]. Remark: as energy content of the ES differs for sPHEV and pPHEV (Table 1), Fig. 6 gives the relation between energy depleted from the ES (ΔW_{ES}^{*}) and $\Delta\mathrm{SOC}$. Marked circle symbols denote the equal data points in Figures. 4, 5 and 6.

Fig. 5 shows energy conversion efficiency of the path from F to L in Fig. 1 (η_{F-L}), energy conversion efficiency of the path from ES to L in Fig. 1 (η_{ES-L}) and effective efficiency of the ICE (η_{ICE}) for a) BUSRTE and b) UDDSHDV drive cycle. At the first sight, Figures 5a and 5b reveal the well-known fact that η_{ES-L} is significantly higher than η_{F-L}, which is mainly related to the fact that η_{ICE} is significantly smaller than unity. However, more

profound analysis is required to distinguish between influences of different powertrain topologies, drive cycles and control strategies.

It can be observed that powertrain electrification results in increased value of η_{ICE}, as downsized ICE in PHEVs can operate in more efficient regions. It can generally be observed that η_{ICE} slightly decreases with increased ΔSOC for pPHEVs. This can be related to the fact that more aggressive depletion of electric energy besides less frequent operation of the ICE also sometimes results in lower ICE loads that are associated with lower ICE efficiency. An opposite trend is observed for the sPHEV especially for the UDDSHDV cycle. This is mainly the consequence of operating the ICE at lower power outputs and thus at lower speeds, which in combination with the high loads means that the engine is operated in the vicinity of the maximum torque and thus in the high efficiency region. However, it should also be noted that although powertrain electrification increases effective efficiency of the ICE, its increase is generally smaller compared to the one observed when electrifying the powertrain of a passenger car as the η_{ICE} of the truck's ICE is already relatively high except for the BUSRTE driven without start-stop strategy (Fig. 5). This fact most significantly influences well-to-wheel CO_2 emissions benefits due to powertrain electrification analyzed in the section 3.3 and it will also lead to different CO_2 emissions trends of the analyzed medium duty truck compared to those published for the passenger cars [8,23].

In addition, it can be observed in Fig. 5 that η_{F-L} of the sPHEV is lower compared to the one of the pPHEV despite higher value of the η_{ICE}. This is generally the consequence of the longer energy conversion chain inherent to series HEVs, since mechanical energy is first transformed to electrical and then back to mechanical energy that is used for propulsion. Longer energy conversion chain of the sPHEV has a significant influence on the overall energy conversion efficiency and thus on the fuel consumption and WtW CO_2 emissions when vehicle is operated in the CS mode. This is very pronounced for the sHEV driven

according to the UDDSHDV cycle as discernible from Fig. 6 and reflected in the results presented in Section 3.3.

Fig. 6 shows energies depleted from both energy storage devices, i.e. ΔW_F and ΔW_{ES}^*, for identical operating conditions as analyzed in Fig. 5. It might be misleading to directly compare only the values of ΔW_F and ΔW_{ES}^*, because η_{F-L} and η_{ES-L} (Fig. 5a and 5b), which represent only TtW efficiency of corresponding on-board energy paths, differ significantly. Therefore it is necessary to consider also WtT CO_2 emissions when analyzing WtW CO_2 emissions. Data of ΔW_F and ΔW_{ES}^*, which are shown in Fig. 6, thus from the basis for the analyses of WtW CO_2 emissions as discernible from Section 2.4 eq. (1).

From Fig. 6a it can be seen that start-stop operation of the ICEV significantly reduces the fuel consumption of the ICEV during the BUSRTE cycle. The reduction is less significant for the UDDSHDV cycle (Fig. 6b) as there are less vehicle stops and the energy consumption for driving the vehicle at higher velocity is larger.

It is also discernible from Fig. 6a that for the BUSRTE cycle both pHEV and sHEV, consume significantly less fuel than ICEV and ICEV_StSt. This is mainly due to notable increase in η_{ICE} (Fig. 5a) and large relative amount of the energy available for regenerative braking (in-depth analysis is given in [9]).

Different trend is observed for the UDDSHDV drive cycle (Fig. 6b) where only parallel pHEV consumes less fuel than both ICEVs, whereas the sHEV consumes more fuel than ICEVs. This is mainly the consequence of relatively high value of η_{ICE} for both ICEVs (Fig. 5b). High value of η_{ICE} of both ICEVs arises from the high average power consumption during the UDDSHDV drive cycle which, due to the drive cycle characteristics and gear shift strategy, favors operation of the ICE in the high efficiency region. In addition, compared to the energy needed for vehicle propulsion, there is less energy available for regenerative

braking over the UDDSHDV drive cycle, which diminishes the positive effect of this fuel consumption reduction mechanism. Both, high value of η_{ICE} in ICEVs and less energy available for regenerative braking lead to only slight improvement in fuel consumption of the pHEV over the ICEV_StSt. Different trend is observed for the series topology, where longer energy conversion chain from the ICE to the wheels that is inherent to the sPHEV increases the fuel consumption of the sHEV above the values of both ICEVs.

For the analyzed case of medium duty truck and UDDSHDV cycle (Fig. 6b) the very small reduction of ΔW_F in case of pHEV, i.e. $\Delta SOC = 0$, over both ICEVs and the increase of ΔW_F value for sHEV reveal significantly different trends compared to the studies related to passenger cars, e.g. [8]. For the passenger cars the increase in efficiency of the ICE due to powertrain hybridization and the regenerative braking generally overcompensate the losses associated with multiple energy conversions and the higher energy demand for powering a heavier vehicle. Therefore in the passenger car segment powertrain hybridization generally leads to the reduction in fuel consumption. In contrast, for the analyzed medium duty truck and UDDSHDV cycle the already high η_{ICE} in the ICEVs provides only limited potential to increase η_{ICE} by powertrain hybridization. This is one of the main reasons for the different fuel consumption trends associated with powertrain electrification between passenger cars and medium duty vehicles.

In addition, Fig. 6 shows that during both drive cycles sPHEV operates in the pure EV mode at maximum value of ΔSOC, which is indicated by the $\Delta W_F = 0$ for maximum value of the ΔSOC. Additionally, it can be observed that EMS control strategy is more efficient for the pPHEV driven according to the BUSRTE as fuel consumption (ΔW_F) of the pPHEV_EMS is smaller than the one of the pPHEV at identical values of ΔSOC as discusses in section 2.3.

Fig. 4 clearly indicates that the depletion rate of the batteries over the drive cycle, i.e. ΔSOC, notably influences the energy efficiency of the powertrain for the UDDSHDV cycle. Therefore, also ΔW_F curves of both topologies do not decrease fully linearly with the increased value of ΔSOC (Fig. 6b) despite slight differences in energy conversion efficiencies of both paths (Fig. 5b). The implications of this important fact will be further discussed in Section 3.3 as it influences WtW CO_2 emissions for the UDDSHDV drive cycle.

3.3. WtW CO_2 emissions

In the following sections WtW CO_2 emissions of the sPHEV and pPHEV are compared for different intensities of electric energy production and for the BUSRTE and for the UDDSHDV drive cycle. For the BUSRTE drive cycle data are shown for sPHEV and for pPHEV with and without EMS controls. For both topologies data are shown for the HEV, i.e. PHEV with $\Delta SOC=0$, and PHEV with maximum depletion rate of the batteries over the drive cycle, which is denoted by the PHEV. These operating points are marked on curve ΔW_F in Fig. 6a with blue squares for the HEV and blue circles for the PHEV. For the UDDSHDV drive cycle data are shown for the sPHEV and the pPHEV without EMS controls strategy as discussed in section 2.3. In addition to the data of the HEV and the PHEV with maximum depletion rate of the batteries over the drive cycle also the data for the intermediate depletion rate of the batteries are analyzed for both topologies. This was done to expose the influence that depletion rate of the batteries in the UDDSHDV drive cycle has on the energy conversion efficiency of the powertrain as discussed in section 3.2. The data for the intermediate depletion rate of the batteries are denoted (PHEV_I) and are marked with blue triangles on the curve ΔW_F in Fig. 6b whereas data for HEV and PHEV are marked with the same symbols as for the BUSRTE. For each of the analyzed cases, Fig. 6 also clearly indicates DoD of the ES over a single BUSRTE and UDDSHDV drive cycle.

The WtW CO_2 emissions values of the ICEV with and without start-stop strategy are summarized in Table 2, whereas they are not shown in the subsequent figures to preserve their readability. Similarly to WtW CO_2 emissions of ICEVs, WtW CO_2 emissions of HEVs (Table 2), i.e. PHEVs with $\Delta SOC = 0$, are also not dependent on the CO_2 intensity of electric energy production. As shown in Fig. 7 WtW CO_2 emissions of HEVs represent the limiting values for the PHEVs for long recharge intervals. The values of HEVs for the BUSRTE cycle indicate that powertrain hybridization of medium duty trucks offers potential for reducing WtW CO_2 emissions in urban driving cycles with frequent vehicle stops already without the option to plug-in to the electrical network. In contrast to the BUSRTE cycle, WtW CO_2 emissions values in the UDDSHDV cycle indicate that, for the analyzed medium duty truck, the powertrain hybridization without the option to plug-in to the electrical network offers very limited potential for reduction of WtW CO_2 emissions in driving cycles that feature a lower potential for replenishing batteries through regenerative braking. Moreover, certain powertrain topologies, i.e. the series one in the analyzed case, can even feature increased WtW CO_2 emissions.

In addition to the notation introduced in section 3, the following notation is used in this section: pPHEV_I - parallel plug-in hybrid electric vehicle operated with the intermediate depletion rate of the batteries and sPHEV_I - series plug-in hybrid electric vehicle operated with the intermediate depletion rate of the batteries.

3.3.1. The case of France

France features the lowest CO_2 intensity of electric energy production analyzed in the paper, which equals to 24.4 gCO_2eq/MJ [32]. Therefore enhanced utilization of the electric propulsion certainly results in low WtW CO_2 emissions as discernible from the Fig. 7a and 7b. It can be clearly seen that for the recharge intervals that fall within the range of the CD

operating mode of the sPHEV, i.e. approx. 20 km, or even for the recharge intervals up to 60 km, the sPHEV offers the lowest value of M_{WtW,CO_2}. This is mainly the consequence of two facts: 1.) sPHEV operates in pure EV mode during CD operation and 2) WtT CO_2 emissions of the electric path are very low in France due to low CO_2 intensity of electric energy production. However, for the recharge intervals longer than 60 km the pPHEV_EMS features the lowest values of M_{WtW,CO_2} for the BUSRTE drive cycle despite the fact that it operates in the blended mode during CD operation. It is discernible from the Fig. 7a that benefits in M_{WtW,CO_2} of the pPHEV_EMS over the sPHEV reach 50g/km for the recharge interval of approximately 90 km, whereas the value increases up to 100 g/km for the recharge interval of approximately 180 km. It can further be seen in Fig. 7a that pPHEV offers only limited possibility to lower the CO_2 emissions when operated in the CD mode compared to the HEV operation as the rate of depletion of batteries of the pPHEV is low for the BUSRTE drive cycle as discussed above.

Similarly as for the BUSRTE drive cycle, sPHEV is preferred solution if recharge intervals are shorter than 60 km also for the UDDSHDV drive cycle due to the facts discussed above, whereas pPHEV is the preferred solution for longer recharge intervals. Unlike the BUSRTE drive cycle, UDDSHDV drive cycle offers the possibility to reduce CO_2 emissions of the PHEVs for longer recharge intervals by adequately controlling the depletion rate of the batteries. It is discernible from Fig. 7b that the CO_2 emissions are lower for larger recharge intervals if intermediate depletion rate of the batteries PHEV_I is applied. This is directly related to the results shown in Fig. 4 and Fig. 6b as fuel consumption curves (ΔW_F) do not decrease fully linearly with the increased value of ΔSOC for the UDDSHDV drive cycle. Therefore, for a certain DoD, operating the PHEV at intermediate depletion rate of the batteries (PHEV_I) as indicated by the triangles in Fig. 6b results in reduced fuel consumption compared to blending the operation of the HEV mode and PHEV mode with

maximum depletion rate of the batteries. Fig. 7b also reveals that benefits due to operating the PHEV at intermediate depletion rate is larger for the pPHEV as it is characterized by a more pronounced curvature of the $W_{F,ES\rightarrow L}$ (Fig. 4). Certainly, operation mode with intermediate depletion rate of the ES does not feature the lowest CO_2 emissions for short recharge intervals, however it might be preferred operation model for longer recharge intervals of the commercial vehicles that frequently feature well defined routes as CO_2 savings might exceed 25 g/km.

As all HEVs feature significantly reduced M_{WtW,CO_2} compared to the ICEVs for the BUSRTE drive cycle it is obvious that also all PHEVs feature lower M_{WtW,CO_2} values for the case of France. Different trend is observed for the UDDSHDV drive cycle, where sHEV features higher M_{WtW,CO_2} value than both ICEVs. Therefore, also both sPHEVs feature lower M_{WtW,CO_2} value compared to the one of the ICEV_StSt only for recharge intervals shorter than approximately 120 km, whereas their M_{WtW,CO_2} value approaches the one of the ICEV for recharge intervals slightly larger than 200 km. This trend is also significantly different compared to the trends for passenger cars that are published in [8,23], where also for long recharge intervals PHEVs always feature lower values of M_{WtW,CO_2}. These vehicle type specific differences are even more pronounced in the subsequent case studies with higher CO_2 intensities of electric energy production.

3.3.2. The case of Europe

Europe features CO_2 intensity of electric energy production that equals to 112.2 gCO_2eq/MJ [32]. Because this value still results in lower WtW CO_2 emissions of the electric propulsion path compared to the fuel propulsion path for all analyzed PHEVs it can be seen in Fig. 7c and 7d that all PHEVs feature lower CO_2 emissions than the HEVs of the same

topology and control strategy. Therefore all analyses related to the trends of the curves given for the case of France are also valid for the results in this section and thus only particular parameters that are specific to this particular CO_2 intensity of electric energy production will be discussed. Two general differences can be observed for the BUSRTE drive cycle compared to the case of France. First, higher CO_2 intensity of electric energy production compared to the case of France significantly diminished potential CO_2 emission reductions of all PHEVs, which is most pronounced for short recharge intervals where vehicles are driven in the CD mode. The second difference arises from the first one and it is related to the reduced recharge interval that allows for the lowest CO_2 emissions of the sPHEV, which comes down to slightly more than 40 km. This is related to the fact that sHEV emits more CO_2 than the pHEV and thus higher CO_2 intensity of electric energy production compared to the case of France less efficiently compensates for this. Both conclusions are also valid for the UDDSHDV drive cycle, where sPHEV features the lowest CO_2 emissions for recharge intervals below approximately 35 km. For the UDDSHDV drive cycle sPHEV features lower M_{WtW,CO_2} value compared to the ICEV_StSt only for recharge intervals shorter than 60 km, and lower M_{WtW,CO_2} value compared to the ICEV for recharge intervals of approximately 100 km.

3.3.3. The case of USA

USA feature CO_2 intensity of electric energy production that equals to 169.6 gCO_2eq/MJ [32]. This increased CO_2 intensity compared to both previous cases results in very interesting trend in the distance specific WtW CO_2 emissions (M_{WtW,CO_2}). It is discernible from Fig 7e that for the BUSRTE drive cycle the trend between sPHEV and sHEV operation is similar as for previously analyzed cases, where it can be noted that the benefit of the sPHEV is smaller also for short recharge intervals due to the increased CO_2 intensity of electric energy

production. Moreover, it can be seen that sPHEV operating in the pure EV mode does not offer the lowest value of M_{WtW,CO_2} for this case. Different as for both previous CO_2 intensity cases and different as for the case of sPHEV, it can be seen that pHEV is more efficient than pPHEV in terms of the WtW CO_2 emissions for this CO_2 intensity of electric energy production. This inverse trend compared to the sPHEV is the consequence of higher efficiency of the energy conversion path from the fuel tank to the load that is characteristic for the parallel topology (Fig. 5a). Due to high fuel economy of the pHEV, for particular values of $E_{WtW,CO_2,F}$ and $E_{WtW,CO_2,EL}$, pHEV operation is more efficient than pPHEV one in terms of the WtW CO_2 emissions as indicated in eq. (1).

Even more interesting trend can be observed for the UDDSHDV drive cycle and the pPHEV. It can be seen from Fig. 7f that similar as for the BUSRTE drive cycle pHEV operation is more efficient than pPHEV operation in terms of the WtW CO_2 emissions, however it can also be seen that operation according to the intermediate depletion rate of the batteries, i.e. pPHEV_I, results in the lowest value of M_{WtW,CO_2}. As already addressed in section 3.3.1 this can be related to the fact that fuel consumption (ΔW_F) curve of the pPHEV does not decrease fully linearly with the increased value of ΔSOC for the UDDSHDV drive cycle (Fig. 6b). Therefore, for a specific range of CO_2 intensities of electric energy production, $m_{WtW,CO_2,dc}$ (eq. (1)) might feature a minimum for operation according to the PHEV_I. This can be explained by two competitive trends. For small values of ΔSOC, $W_{F,ES\rightarrow L}$ significantly decreases with increased ΔSOC (Fig. 4) and efficiencies of both energy conversion paths (Fig. 5b) do not change significantly. Therefore, reduction in fuel consumption and thus in $\Delta W_F E_{WtW,CO_2,F}$ (eq. (1)) is larger as increase in $\Delta W_{ES}^{*} E_{WtW,CO_2,EL}$ (eq. (1)) due to depletion of the batteries. However, for higher values of ΔSOC the $W_{F,ES\rightarrow L}$ does not reduce significantly and thus negative influences of $\Delta W_{ES}^{*} E_{WtW,CO_2,EL}$ due to high CO_2

intensities of electric energy production prevail. This case clearly indicates the importance of applying adequate control strategies. M_{WtW,CO_2} of the sPHEV features similar trend as for the both previously analyzed CO2 intensity cases, whereas it can be observed that the benefit of the sPHEV is smaller due to higher value of CO_2 intensity of electric energy production. For the case of the USA all series topologies feature larger value of M_{WtW,CO_2} compared to the ICEV_StSt.

Fig. 7e and 7f also indicate that this CO_2 intensity of electric energy production presents an approximate threshold value that favors the operational switch from CD to CS for the analyzed vehicle. Fig. 7e shows that for BUSRTE, pPHEVs feature lower M_{WtW,CO_2} values in the HEV mode and thus for this particular vehicle and for this particular operation threshold value is slightly below 169.6 gCO_2eq/MJ. Fig. 7f shows a mixed M_{WtW,CO_2} trend for UDDSHDV and pHEVs, which depends on the control strategy. Therefore 169.6 gCO_2eq/MJ indeed represents a threshold value for this case. It can be observed that sPHEV features lower M_{WtW,CO_2} values compared to the sHEV for both drive cycles, whereas the difference is more pronounced for short recharge intervals. Therefore, the threshold value of the CO_2 intensities of electric energy production lies slight above the 169.6 gCO_2eq/MJ for the sPHEV and both drive cycles. These results are clearly in contrast to the results of the study on passenger cars published in [23], where it is shown that for the same intensity of electric energy production the enhanced depletion of electric energy is clearly favored for reducing WtW CO_2 emissions.

3.3.4. The case of China

China features CO_2 intensity of electric energy production that equals to 241.1 gCO_2eq/MJ [32]. As discernible from Fig. 7g and 7h it can be concluded that high CO_2

intensity of electric energy production does not favor the operation in the CD mode for both drive cycles and for both PHEV topologies as M_{WtW,CO_2} values of PHEVs are always larger compared to the ones of the corresponding HEVs. Out of all PHEVs driven according to both drive cycles the pPHEV_I driven according to the UDDSHDV drive cycle might be considered as the only exception as it features only slightly increased value of M_{WtW,CO_2} compared to the corresponding HEV due to the facts discussed in section 3.3.3.

4. Conclusions

Well-to-Wheel CO_2 emissions of different powertrain topologies employed in powering a medium duty truck are analyzed in the paper. Analysis is performed for the parallel and series PHEV topology which are driven according to two drive cycles with significantly different characteristic. In addition, different control strategies of operating the parallel PHEV were investigated for the BUSRTE drive cycle. In addition to the operation of the vehicle in the plug-in mode, the vehicle was also operated only in the charge sustaining mode thus giving the Well-to-Wheel CO_2 emissions of a HEV equivalent. Furthermore, all these topologies were compared to the baseline ICEV operated with and without the start-stop strategy. Due to the need to adequately model the various topologies, a forward facing system simulation model incorporating a mechanistic engine sub-model was used. The simulation results give, on one hand, the input data for the Well-to-Wheel CO_2 emissions analysis and, on the other hand, provide the insight into the energy conversion phenomena of powertrains that is required for the in-depth analysis.

Based on these data Well-to-Wheel CO_2 emissions are analyzed for four different realistic CO_2 intensities of electric energy production. Main findings can be summarized in:

1. High efficiency values of the internal combustion engines in trucks require careful analysis before introducing electric hybridization and plug-in hybridization of these vehicles. Therefore certain HEV topologies might not be competitive to the ICEVs in terms of Well-to-Wheel CO_2 emissions. Moreover, PHEVs might also not be able to compensate for this deficiency even for short recharge intervals if CO_2 intensities of electric energy production are not sufficiently low. Generally, the higher efficiency values at which the internal combustion engines operate in trucks provide, compared to passenger cars, a smaller margin for reduction of Well-to-Wheel CO_2 emissions on the account of propulsion electrification.
2. The highest benefits of HEVs in terms of Well-to-Wheel CO_2 emissions can be achieved in the drive cycles featuring frequent decelerations enabling substantial energy recuperation by regenerative braking.
3. For driving cycles with less vehicle stops parallel HEV topology performs better than the series one, however the Well-to-Wheel CO_2 emissions benefit due to powertrain electrification is much smaller compared to urban driving cycles.
4. Low CO_2 intensities of electric energy production favor operation of the PHEVs in the charge depleting mode and preferably in the pure EV mode, whereas high CO_2 intensities favor operation in the charge sustaining mode. The threshold value of the CO_2 intensities of electric energy production that results in the operational switch is lower for the trucks compared to the passenger cars.
5. Low CO_2 intensities of electric energy production favor pure EV operation in the charge depleting mode for short recharge intervals. For longer recharge intervals operation in the blended mode with less intensive depletion rate of the electric storage devices features the lowest Well-to-Wheel CO_2 emissions even for low CO_2 intensities of electric energy production.

For the analyzed medium duty truck it can thus be concluded that for both driving cycles low CO_2 intensity of electric energy production and operation in the full EV mode, i.e. SPHEV, certainly offers the lowest Well-to-Wheel CO_2 emissions for short recharge intervals, whereas for longer recharge intervals operation of the parallel configuration in the blended mode is preferred. Results presented in the paper clearly indicate that it is necessary to profoundly analyze the interaction between vehicle parameters, powertrain topology, its control strategy, component characteristics and sizes, envisaged drive cycle and recharge options together with the CO_2 intensity of electric energy production to get most of powertrain electrification, as powertrain electrification not necessarily results in lower Well-to-Wheel CO_2 emissions especially in the medium truck segment.

References

[1] Lukic SM, Emadi A. Effect of drivetrain hybridization on fuel economy and dynamic performance of parallel hybrid electric vehicles. IEEE transactions on vehicular technology 2004. 53/2, 385-389.

[2] Lee H, Kim H. Improvement in fuel economy for a parallel hybrid electric vehicle by continuously variable transmission ratio control. Proc. Instn. Mech. Engrs., Part D, J. of Automotive Engineering 2005, 219, 43-51.

[3] Albert IJ, Kahrimanovic E and Emadi A. Diesel sport utility vehicles with hybrid electric drive trains. IEEE transactions on vehicular technology 2004. 53/4, 1247-1256.

[4] Tyrus JM et al. Hybrid electric sport utility vehicles. IEEE transactions on vehicular technology 2004. 53/5, 1607-1622.

[5] Katrašnik T. Energy Conversion Efficiency of Hybrid Electric Heavy-duty Vehicles. SAE Technical Paper 2009-01-1867, 2009.

[6] Banjac T, Trenc F, Katrašnik T. Energy conversion efficiency of hybrid electric heavy-duty vehicles operating according to diverse drive cycles. Energy Convers. Manage. 2009, 50, 2865–2878.

[7] Quinn C, Zimmerle D, Bradley TH. The effect of communication architecture on the availability, reliability, and economics of plug-in hybrid electric vehicle-to-grid ancillary services. Journal of Power Sources 2010. 195, 1500–1509.

[8] Norman Shiau CS, Samaras C, Hauffe R, Michalek JJ. Impact of battery weight and charging patterns on the economic and Environmental benefits of plug-in hybrid vehicle. Energy Policy 2009. 37, 2653–2663.

[9] Katrašnik T. Energy conversion phenomena in plug-in hybrid-electric vehicles. Energy Convers. Manage. 2011. 52, 2637-2650.

[10] Sioshansi R, Denholm P. Emissions Impacts and Benefits of Plug-In Hybrid Electric Vehicles and Vehicle-to-Grid Services. Environ. Sci. Technol. 2009. 43, 1199–1204.

[11] Stephan CH, Sullivan J. Environmental and Energy Implications of Plug-In Hybrid-Electric Vehicles. Environ. Sci. Technol. 2008. 42, 1185–1190.

[12] Samaras C, Meisterling K. Life Cycle Assessment of Greenhouse Gas Emissions from Plug-in Hybrid Vehicles: Implications for Policy. Environ. Sci. Technol. 2008. 42, 3170–3176.

[13] Silva C, Ross M, Farias T. Evaluation of energy consumption, emissions and cost of plug-in hybrid vehicles. Energy Convers. Manage. 2009. 50, 1635–1643.

[14] Silva C. Electric and plug-in hybrid vehicles influence on CO2 and water vapour emissions. International Journal of Hydrogen Energy. 2011. 36, 13225-13232.

[15] Andress D, Nguyen TD, Das S. Reducing GHG emissions in the United States' transportation sector. Energy for Sustainable Development. 2011. 15, 117–136.

[16] Axsen J, Kurani KS, McCarthy R, Yang C. Plug-in hybrid vehicle GHG impacts in California: Integrating consumer-informed recharge profiles with an electricity-dispatch model. Energy Policy. 2011, 39, 1617–1629.

[17] Lemoine DM, Kammen DM, Farrell AE. An innovation and policy agenda for commercially competitive plug-in hybrid electric vehicles. Environ. Res. Lett. 2008, 3, 014003 (10pp).

[18] van Vliet O, Brouwer AS, Kuramochi T, van den Broek M, Faaij A. Energy use, cost and CO_2 emissions of electric cars. Journal of Power Sources, 2011. 196, 2298–2310.

[19] Thiel C, Perujo A, Mercier A. Cost and CO_2 aspects of future vehicle options in Europe under new energy policy scenarios. Energy Policy. 2010. 38, 7142–7151.

[20] van Vliet O, Kruithof T, Turkenburg WC, Faaij A. Techno-economic comparison of series hybrid, plug-in hybrid, fuel cell and regular cars. Journal of Power Sources. 2010. 195, 6570–6585.

[21] Sioshansi R, Fagiani R, Marano V. Cost and emissions impacts of plug-in hybrid vehicles on the Ohio power system. Energy Policy. 2010. 38, 6703–6712.

[22] Varnhagen S, Same A, Remillard J, Park JW. A numerical investigation on the efficiency of range extending systems using Advanced Vehicle Simulator. Journal of Power Sources, 2011. 196, 3360–3370.

[23] Doucette RT, McCulloch MD. Modeling the prospects of plug-in hybrid electric vehicles to reduce CO_2 emissions. Applied Energy. 2011, 88, 2315-2323.

[24] Katrašnik T. Hybridization of powertrain and downsizing of IC engine - a way to reduce fuel consumption and pollutant emissions - Part 1. Energy convers. manage, 2007. 48/5, 1411-1423.

[25] Katrašnik T, Trenc F, Rodman Oprešnik S. Analysis of the Energy Conversion Efficiency in Parallel and Series Hybrid Powertrains. IEEE transactions on vehicular technology, 2007, 56, 6/2, 3649-3659.

[26] Katrašnik T. Hybridization of powertrain and downsizing of IC engine - Analysis and parametric study - Part 2. Energy convers. manage, 2007. 48/5, 1424-1434.

[27] Katrašnik T. et al. Improvement of the dynamic characteristic of an automotive engine by a turbocharger assisted by an electric motor. J. eng. gas turbine power, 125, 2, 2003, 590-595.

[28] Pacejka HB. Tire and Vechicle Dynamics. SAE International, Second edition, 2006.

[29] National Renewable Energy Laboratory. ADVISOR Documentation.

[30] EPA. Accessed November 2012 from: http://www.epa.gov/nvfel/testing/dynamometer.htm

[31] EC JRC. Well-to-Wheels analysis of future automotive fuels and powertrains in the European context. Report Version 3c, July 2011.

[32] CARMA. National CO_2 Intensity Data. Accessed May 2012 from: www.carma.org.

[33] Ehsani M, Gao Y, Emadi A. Modern electric, hybrid electric, and fuel cell vehicles: fundamentals, theory, and design, CRC Press: Taylor & Francis, 2010.

[34] Katrašnik T. Analytical framework for analyzing the energy conversion efficiency of different hybrid electric vehicle topologies. Energy Convers. Manage. 2009. 50, 1924-1938.

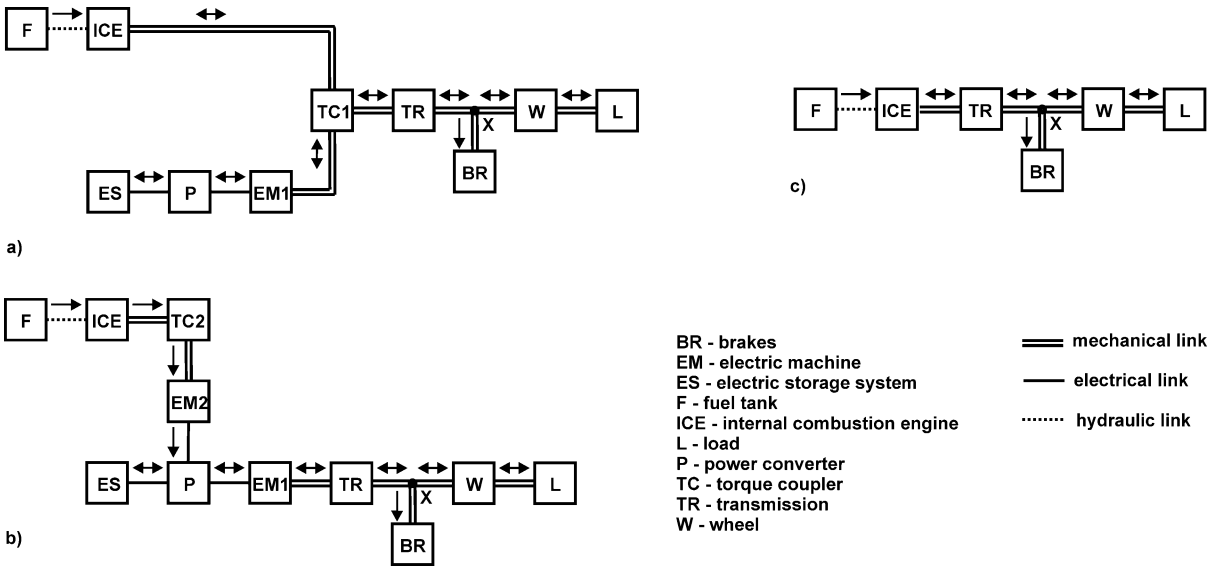

Fig. 1 (a) Parallel and (b) series PHEV topology, and c) ICEV topology with indicated energy paths. Energy is added to the ICEV and parallel and series HEV only by the fuel (F), whereas parallel and series PHEV are also charged from an electric grid (ES).

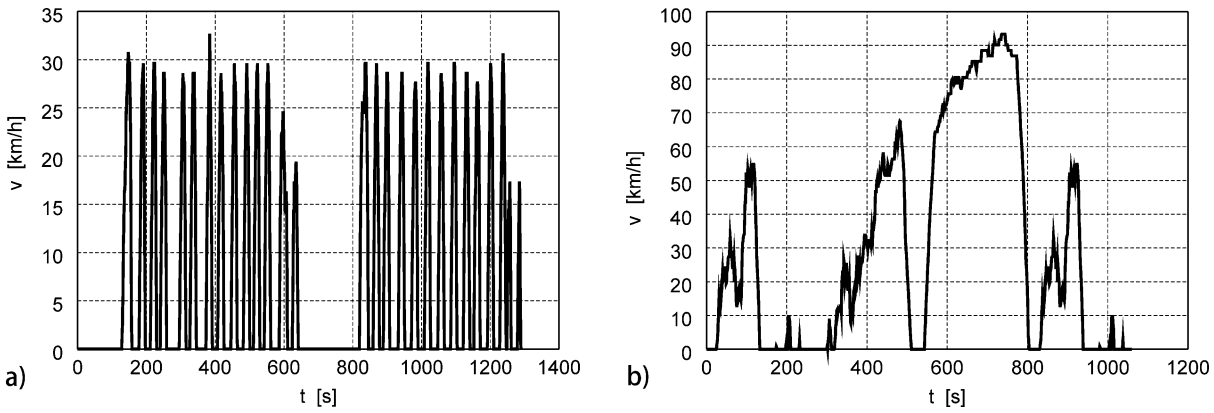

Fig. 2 Velocity profile of: (a) BUSRTE, and (b) UDDSHDV drive cycles

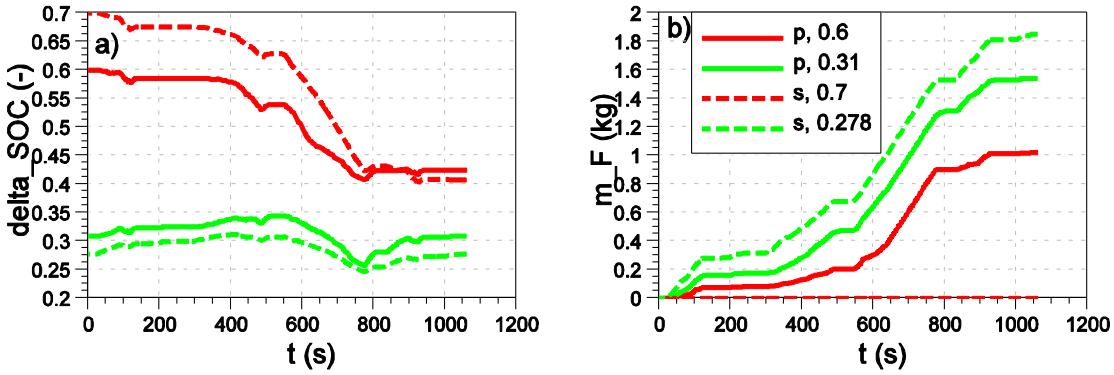

Fig. 3 (a) ΔSOC and (b) mass of the fuel consumed over the drive cycle ($m_{F,dc}$) of the pPHEV and sPHEV driven according to the UDDSHDV drive cycle for different initial values of the SOC

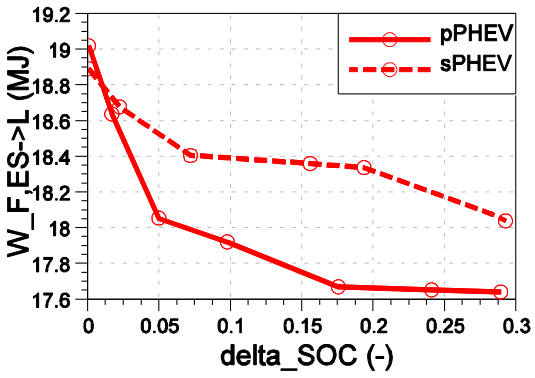

Fig. 4 $W_{F,ES\rightarrow L}$ of pPHEV and sPHEV driven according to the UDDSHDV drive cycle for different depletion rates of the electric storage devices

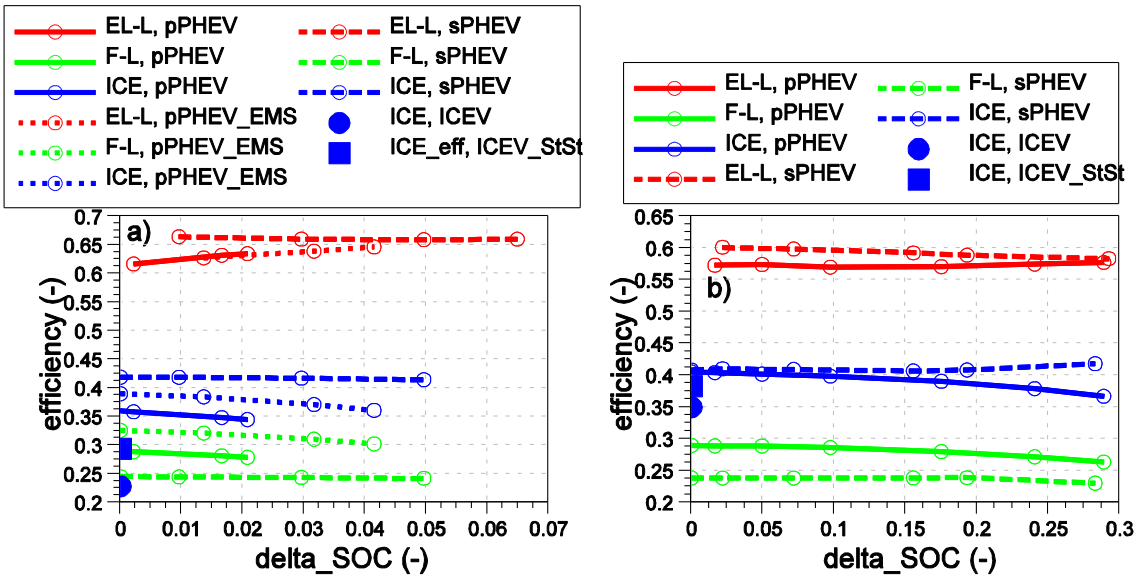

Fig. 5 Energy conversion efficiency of the path from F to L (η_{F-L}), energy conversion efficiency of the path from ES to L (η_{ES-L}) and effective efficiency of the ICE (η_{ICE}) of different powertrain topologies driven according to the (a) BUSRTE and (b) UDDSHDV drive cycle

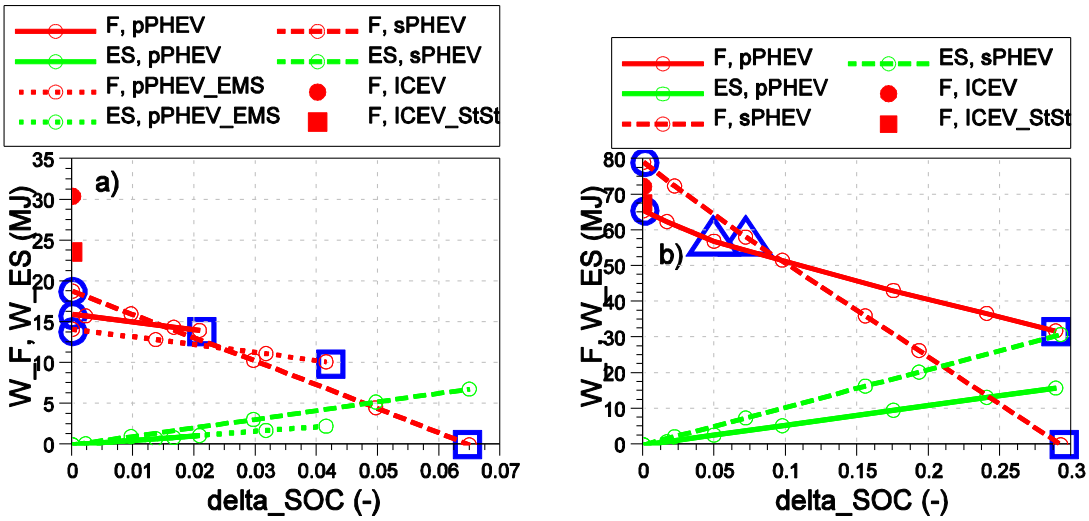

Fig. 6 Energy depleted from the fuel tank (ΔW_F) and energy depleted from the batteries (ΔW_{ES}^*) of different powertrain topologies driven according to the (a) BUSRTE and (b) UDDSHDV drive cycle

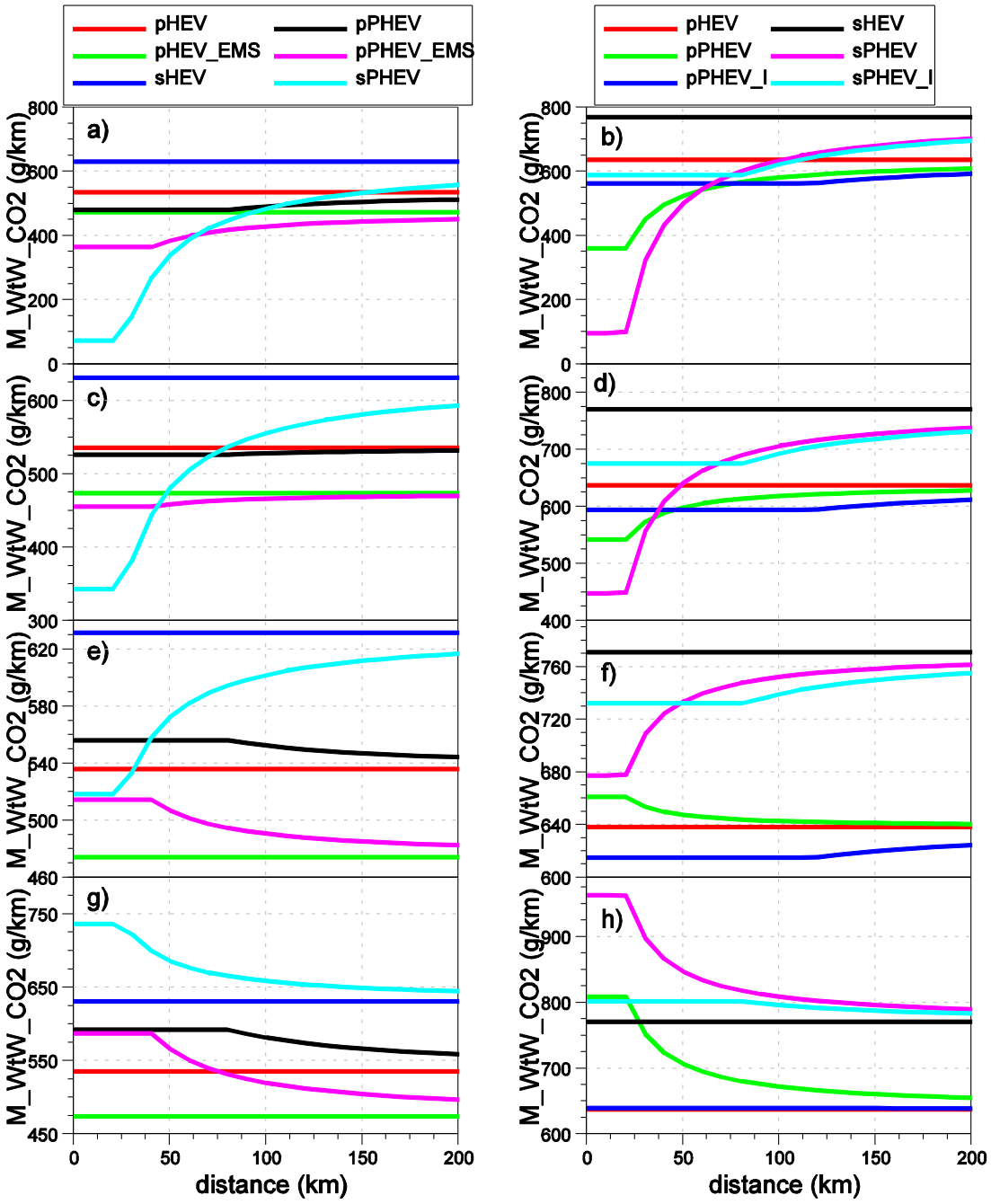

Fig. 7 WtW CO2 emissions (M_{WtW,CO_2}) for the case of France – (a) BUSRTE and (b) UDDSHDV drive cycle; for the case of Europe – (c) BUSRTE and (d) UDDSHDV drive cycle; for the case of USA – (e) BUSRTE and (f) UDDSHDV drive cycle; and for the case of China – (g) BUSRTE and (h) UDDSHDV drive cycle. To preserve space in axis notation (g/km) is used to represent (gCO_2eq/km).

Table 1 Basic ICEV and PHEV data

	ICEV	sPHEV	pPHEV
m_V [kg]	7490	8062	7755
Frontal area [m^2]		5.66	
Drag coefficient [-]		0.7	
P_{ICE} [kW]	162	77.5	77.5
P_{EM1} [kW]	-	126.4	67.1
P_{EM2} [kW]	-	94.6	-
W_{ES} [kWh]	-	29.4	15.4
$t_{0-50km/h}$ [s]	10.44	13.1	8.25
$t_{0-100km/h}$ [s]	39	51.1	39.4

Table 2 WtW CO_2 emissions of ICEVs and HEVs, i.e. PHEVs with $\Delta SOC = 0$, in (gCO_2eq/km)

	BUSRTE	UDDSHDV
ICEV	1047	722
ICEV_StSt	812	675
pHEV	549	654
pHEV_EMS	486	-
sHEV	647	790